



# Impact of electric vehicles fast frequency regulation and charging strategies on grid frequency stability

A. Ordone<sup>1</sup>, F.J Asensio<sup>1</sup>, J.I. San Martín<sup>1</sup>, M. González-Pérez<sup>1</sup> and J.A. Cortajarena<sup>2</sup>

<sup>1</sup> Department of Electrical Engineering  
Engineering School of Gipuzkoa (Eibar), University of the Basque Country  
Avda. Otaola, 29, 20600 Eibar (Spain)  
Phone/Fax number: +34 943 033036, e-mail: [ander.ordono@ehu.es](mailto:ander.ordono@ehu.es)

<sup>2</sup> Department of Electronic Technology  
Engineering School of Gipuzkoa (Eibar), University of the Basque Country  
Avda. Otaola, 29, 20600 Eibar (Spain)

**Abstract.** With the gradual reduction of grid inertia, system sensitivity to load unbalances is increasing, compromising frequency stability. To face this problem, faster frequency regulation resources are required. In this context, vehicle-to-grid (V2G) is one of the concepts that is suggested for this purpose. When electric vehicles (EVs) are parked, their batteries can be used as distributed energy storage systems (EESs), injecting and absorbing power faster than conventional generation units (CGUs). The goal of this paper is to analyse the impact of fast frequency regulation of EVs in a small-scale grid, under sudden load variations. In this paper, the effect of charging strategies (CSs) is addressed, as they have a direct impact on the magnitude of the EV fleet regulation. In this way, different CSs can be used to achieve symmetrical up and down regulation, or to maximize one of them. The effect of the EV fleet dynamics in the frequency transient is also studied. The speed of response, and hence, the frequency transient, are influenced by these dynamics. The focus of the analysis will be the communication delay between the EV fleet and the central controller.

**Key words.** V2G, fast frequency regulation, electric vehicle, charging strategies, frequency response.

## 1. Introduction

In recent years, the share of renewable energy sources (RES) in the electricity generation mix has increased. These resources have led to a more environmentally friendly power grid. However, the change in the generation paradigm has brought new challenges. On the one hand, the replacement of CGUs by converter-based RES is reducing the overall inertia of the grid [1]. This effect is further increased due to the use of HVDC links. On the other hand, RES stochastic behaviour makes it difficult to match the generated and consumed power. In this low-inertia scenario, a small unbalance in the power could generate a high rate of change of frequency (RoCoF). As CGUs require some seconds to adapt their power, a high RoCoF could lead to an excessive frequency deviation, producing a system collapse [2].

The conventional approach to manage the active power balancing has been the frequency control/reserve (FR) [3]. In this regulation, some generators and loads adapt their

power output to keep the system balanced. As shown in Figure 1, the FR is composed of the inertial response and three reserves, which depend on the timescale and the reaction time. From faster to slower: frequency containment reserve (FCR), frequency restoration reserve (FRR) and replacement reserve (RR). As the inertia of the grid is reduced, new FR services have been suggested to provide support before the FCR. Two examples are Inertia Emulation (IE) and Fast Frequency Regulation (FFR) [4]. FFR has recently started as an open market in Great Britain and Nordic grids [5]. It usually requires response times below 1-2 s, which fit the converted-based generation system. In this context, stationary EESs, such as batteries (BESS) have gained popularity in this service.

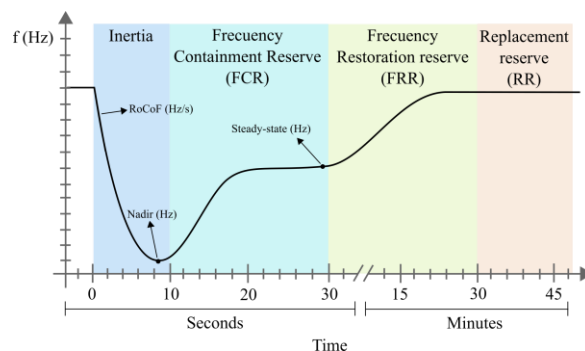


Figure 1. Frequency regulation stages under a load increase

On the meantime, the number of EVs that are available around the world is increasing [6]. The main function of EVs is to meet user displacement requirements. However, as they are parked 95% of the time, they can be used as distributed BESS connected to the grid. V2G has emerged as an interesting solution to improve grid quality and provide economic revenues to the vehicle owners. If EVs are properly grouped/aggregated, they can contribute to several ancillary services by injecting or absorbing power from the grid [7]. Among the ancillary services, FCR, and specially FFR, have been envisioned as the most profitable ones due to the high power and low energy requirements [8]. The impact of EVs on the frequency stability is a topic

of research in recent years [9]–[11], but it still requires further investigation.

This paper is focused on the impact of EVs FFR regulation on the frequency stability of low inertia grids. The novel contribution of this work is to evaluate the impact of 1) the charging strategy and EV availability on the magnitude response and 2) the EV fleet and controller dynamics on the transient response, focusing on communication delays.

## 2. FCR & FFR theoretical approach

Among FR services (Figure 1), FCR is the fastest service to actuate. Its goal is to stop the grid frequency deviation under a power unbalance. Then, FRR and RR will slowly restore the frequency to the rated value. FFR is similar to FCR, but with faster activation times. The relation between the grid frequency and the power is given by a variation of the swing equation [2]:

$$\frac{2H}{\omega_s} \frac{d\omega_s}{dt} = P_m - P_e \quad (1)$$

The equation is given in per unit basis:  $H$  is the inertia constant of the system in seconds,  $\omega_s$  is the angular speed of the grid in rad/s, and  $P_m$  and  $P_e$  are the generators and consumers power respectively, in pu. As the angular speed  $\omega_s$  and the grid frequency  $f$  are directly related, both terms will be used indistinctly during this analysis.

For small perturbations around the nominal operating point, denoted with the subscript 0, the previous equation can be rewritten as (2), and it can be simplified to (3) considering an equilibrium point:

$$\frac{2H}{\omega_{s0}} \frac{d(\omega_{s0} + \Delta\omega_s)}{dt} = P_{m0} - P_{e0} + \Delta P_m - \Delta P_e \quad (2)$$

$$\frac{2H}{\omega_{s0}} \frac{d(\Delta\omega_s)}{dt} = \Delta P_m - \Delta P_e \quad (3)$$

Assuming that the FCR is only provided by generators,  $\Delta P_m$  can be divided in three components, as shown in (4): 1) a dispatched or uncontrolled term,  $\Delta P_m'$ ; 2) A droop component which modifies the generated power according to angular speed deviation  $\Delta\omega_s$  and the droop coefficient  $R$ , which is the base of FCR; 3) An IE component that mimics inertia behaviour, which is proportional to the grid angular speed derivative  $d\Delta\omega_s/dt$  and the synthetic inertia term  $H_v$ .

$$\Delta P_m = \Delta P_m' - \frac{1}{R} \cdot \Delta\omega_s - \frac{2H_v}{\omega_{s0}} \cdot \frac{d\Delta\omega_s}{dt} \quad (4)$$

For the consumed power (5), two components are identified: 1) a dispatched or uncontrolled load term,  $\Delta P_e'$ , and 2) a component proportional to the frequency deviation, which models the damping effect of the load. This term is generally related to pumps, fans or electric motors directly coupled to the grid, whose power is proportional to the frequency. In (5),  $D$  refers to the load damping factor, in pu/(rad/s).

$$\Delta P_e = \Delta P_e' + D \cdot \Delta\omega_s \quad (5)$$

Replacing (4) and (5) in (3), the equations for the grid angular speed derivative (6) and steady state value (7) under a power unbalance are obtained.

$$\frac{d\Delta\omega_s}{dt} = \frac{\omega_s}{2} \frac{\Delta P_m' - \Delta P_e' - (1/R + D)\Delta\omega_s}{H + H_v} \quad (6)$$

$$\Delta\omega_s = \frac{\Delta P_m' - \Delta P_e' - \frac{2}{\omega_s}(H + H_v) \frac{d\Delta\omega_s}{dt}}{1/R + D} \quad (7)$$

Both droop and synthetic inertia coefficients appear in the previous equations. However, RoCoF is mainly influenced by the inertia, whereas droop constant determines the steady state frequency deviation. It should also be noted that the reaction of the droop regulation is not immediate due to the dynamics of the generators, and hence, the frequency transient will also be impacted by these dynamics.

## 3. System model

The modelled grid is based on the island of Bornholm, Denmark. This grid can be operated in islanded mode or connected to the main grid. In islanded mode, system inertia is small and FCR is provided mainly by a slow CGU steam turbine [9]. The key parameters are gathered in Table 1. A base power of 25 MVA is used for pu values. The simplified diagram is shown in Figure 2.

Table 1. System model parameters. In brackets, values in international system (IS) units.

	Parameter	Value
Grid	Inertia ( $H$ )	4.3 s (2564 kg m <sup>2</sup> )
	Damping factor ( $D$ )	1.5 pu / Hz (0.38 MW/Hz)
	Rated power ( $P_{g0}$ )	1 pu (25 MW)
	Droop coefficient ( $R_t$ )	0.03 (0.06 Hz/MW)
	FCR @ 100 mHz	0.067 pu (1.667 MW)
CGU	Speed governor time constant ( $T_g$ )	0.2 s
	Prime mover time constant ( $T_t$ )	0.3 s

### A. Grid model

The grid is modelled as a first order transfer function. Using equations (3) and (5) in the Laplace domain, and renaming  $\Delta P_m - \Delta P_e'$  as the net power variation  $\Delta P_{net}$ , (8) is obtained:

$$\frac{\Delta\omega_s}{\Delta P_{net}} = \frac{\omega_s}{2Hs + \omega_s D} \quad (8)$$

According to the previous equation, grid frequency depends on the load damping coefficient, the inertia and the net active power.

### B. CGU model

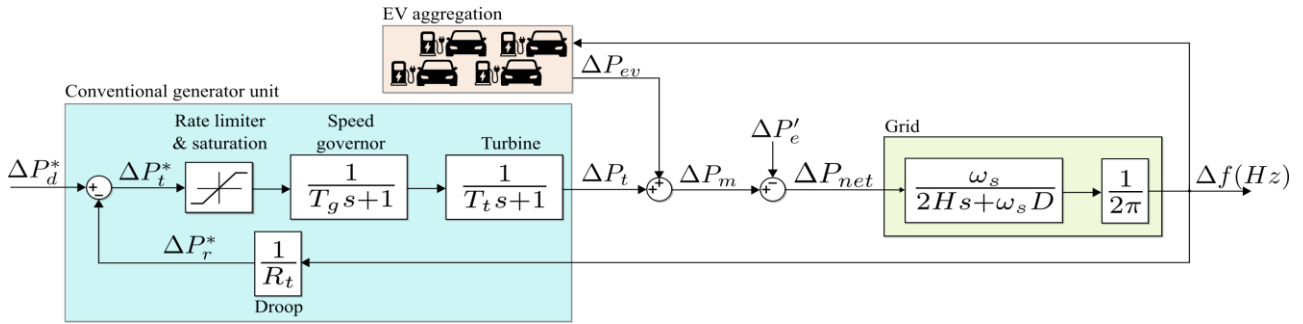


Figure 2. Grid model for evaluating FCR capability, including EV aggregation and CGU

The CGU model is highlighted in blue in Figure 2. A rate limiter & saturation block is used to limit the maximum frequency regulation power to 0.067 pu. The power setpoint rate of change is not limited.

The CGU dynamics are modelled using two first order transfer functions. The first one models the response of the speed governor, which is dominated by the time constant of the servomotor,  $T_g$ . The second one corresponds to the response of the turbine, which is modelled according to its mechanical time constant  $T_t$ .

FCR is carried out using a droop-based feedback control. The droop controller will modify the dispatched power by the CGU  $\Delta P_d^*$  with a frequency dependant component  $\Delta P_r^*$ . The droop coefficient  $R_t$  determines the ratio between the frequency and power variation (9):

$$R_g = \frac{\Delta f / f_0}{\Delta P_d^* / P_{g0}} \quad (9)$$

Where  $P_{g0}$  is the rated power of the CGU (pu),  $f_0$  is the rated grid frequency (Hz),  $\Delta f$  is the frequency deviation and  $\Delta P_d^*$  is the droop controller output.

### C. EV fleet model

As the power and energy of a single EV is limited, they must be aggregated or grouped to participate in ancillary services. This paper considers a 50 EV fleet with V2G charging points located at owner's houses. The EV fleet characteristics are summed up in Table 2. The plug-in time, plug-out time and required charge are obtained considering uniform distributions.

Table 2. EV aggregation model parameters

Parameter	Value
Number of EVs ( $n_{ev}$ )	50
Power of the charger ( $P_{ev0}$ )	$\pm 0.004$ pu ( $\pm 10$ kW)
Plug-in time ( $t_{plug\ in}$ )	Uniform (7:00, 9:00) h
Plug-out time ( $t_{plug\ out}$ )	Uniform (18:00, 21:00) h
Required charge (DoD)	Uniform (50, 80) %
Battery capacity ( $C_{bat}$ )	40 kWh
Measuring time constant ( $T_m$ )	0.1 s
EV time constant ( $T_{ev}$ )	0.1 s
Communication delay ( $T_c$ )	0.1 s

The simplified diagram for the fleet is represented in Figure 3. This study considers a central controller to manage the

FFR. The central controller uses the measured grid frequency deviation, the vehicles current charging power  $P_c$  and rated charger power  $P_{ev0}$  to calculate the overall EV fleet FFR power using a dynamic droop. The overall power setpoint is shared according to each EV available FR capability.

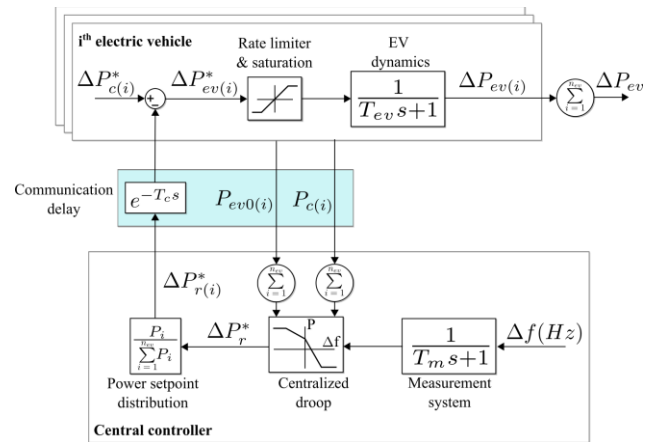


Figure 3. Model for the EV fleet with a central controller

The proposed dynamic droop is shown in Figure 4. A negative power refers to battery charging. Two different droop coefficients are identified, one for up regulation (overload) and the other for down regulation (underload). These coefficients are calculated according to the EVs overall charging power and charging station rated capacity.  $|\Delta f|_m$  is set to 0.1 Hz. The frequency dead band  $|\Delta f|_{db}$  is ignored in this study.

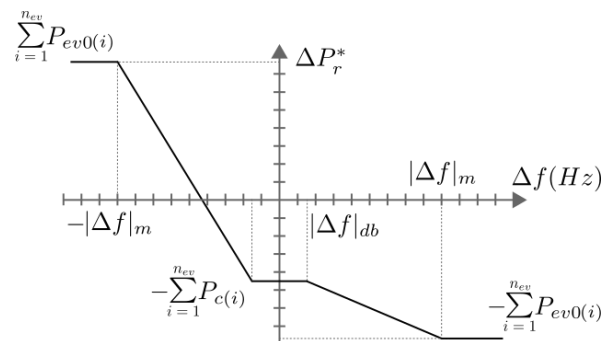


Figure 4. Proposed dynamic droop controller

The dynamics of the measuring system and EV charging stations are modelled using a first order transfer function with  $T_m$  and  $T_{ev}$  time constants, respectively. Local controllers usually require a frequency measuring window between 0.1 and 0.2 s [12]. Charging station dynamics range between 30 to 100 ms [13]. The communication

between the EVs and the central controller is modelled with a single delay  $T_c$ .

The following assumptions are considered for the EV fleet: 1) power conversion efficiency is 100%. 2) EVs are not fully charged nor discharged when plugged. FFR is always available. 3) As FFR operating time is short ( $< 30$  s), its impact on battery charge is neglected.

#### 4. Simulation results

The impact of FFR in the dynamic response is evaluated measuring RoCoF and maximum frequency deviation. The steady-state frequency deviation is used to evaluate the static behaviour:

- RoCoF (Hz/s): Obtained using (10), it is the grid frequency slope measured in a 500 ms window [12].  $f'$  is the frequency 500 ms after the load perturbation.

$$RoCoF = \frac{\Delta f}{\Delta t} = \frac{f' - f_0}{0.5} \quad (10)$$

- $\Delta f_{\max}$  (Hz): Maximum frequency deviation during the frequency transient.
- $\Delta f_s$  (Hz): Steady-state frequency deviation. Frequency deviation after the transient.

##### A. Impact of charging strategies

The simulations have been carried out considering two charging strategies for the EV fleet. Both strategies start the charging process at 22:00, which is the typical start hour of the off-peak period  $t_{op}$ :

- CS 1 - Full power charge: Charger rated power is used during the charging process. It provides the highest charging efficiency [14], but the regulation down capability is lost during this process.
- CS 2 - Minimized power charge: Charging power depends on the time that the EV is plugged (11). This strategy prevents overloading under high EV penetration. It also provides higher symmetry for regulation up and down capability.

$$P_c = \frac{C_{bat} \cdot DoD}{t_{plug\ out} - t_{op}} \quad (11)$$

The FFR capacity for the charging strategies during a 24 h period is shown in Figure 5. Both regulation up and regulation down capabilities are considered. Negative power refers to regulation down capacity (power absorbed by the EVs).

The FFR capacity depends on the EVs availability. It is maximized from 21:00 to 7:00, when all the EVs are plugged. No regulation can be provided from 9:00 to 18:00. The maximum capacity is achieved during charging process of CS 1 (22:00 to 24:00 approx.), with a 4% up regulation, but without down regulation. On the other hand, CS 2

provides an additional 2.5% up regulation and 1.5% down regulation to the grid when all the EVs are plugged.

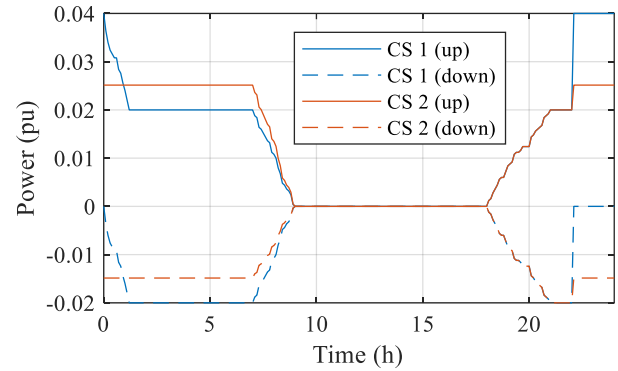


Figure 5. FFR capacity of EV fleet for different charging strategies. The results are given for a 24 h period.

The frequency deviations and RoCoF results for a 1.5% load perturbation  $\Delta P_e'$  is shown in Figure 7. Charging strategies compared with the base case where no EVs are available. The load unbalance is tested at different times.

Both EV fleet availability and charging strategy have a direct impact on the transient and steady-state response. The achieved frequency deviations and RoCoF are closely related to the FFR capacity of the EV fleet (Figure 5), and hence, the shape is shared. The grid frequency stability is improved at nights, when the EV fleet is connected. However, from 9:00 to 18:00 the stability only depends on the FCR of the CGU. EVs FFR could also be available during the day if charging stations were considered in working places and public locations.

Under a load increase during the charging period of CS 1,  $|\Delta f_s|$ ,  $|\Delta f_{\max}|$  and  $|RoCoF|$  can be improved by 37%, 24.6% and 15.1%, respectively. However, no improvement is achieved during a load decrease. Once the charging is completed, the vehicles are plugged without consuming power from the grid. Symmetrical regulation up and down is provided during this time. With the 50 EVs connected, the improvement for the previous parameters is 22.7%, 15.5% and 7.5% respectively.

For the CS 2 strategy, up regulation is somewhat higher than down regulation. However, unlike CS 1, it is always available. During regulation up,  $|\Delta f_s|$ ,  $|\Delta f_{\max}|$  and  $|RoCoF|$  can be improved 27.2%, 18.2% and 9.6%. In regulation down, they are reduced to 18.1%, 12.3% and 5.6%.

EVs FFR has a bigger impact in the frequency deviations ( $\Delta f_{\max}$  and  $\Delta f_s$ ). The RoCoF, as it was mentioned in section 2, is highly dependent on grid inertia and other techniques such as IE are required to improve it.

##### B. Impact of the communication delay

The frequency transient is determined by the load unbalance size, the available grid inertia and the speed and magnitude of the response. The impact of the magnitude of the response has already been carried out in the previous section, considering EVs availability and charging

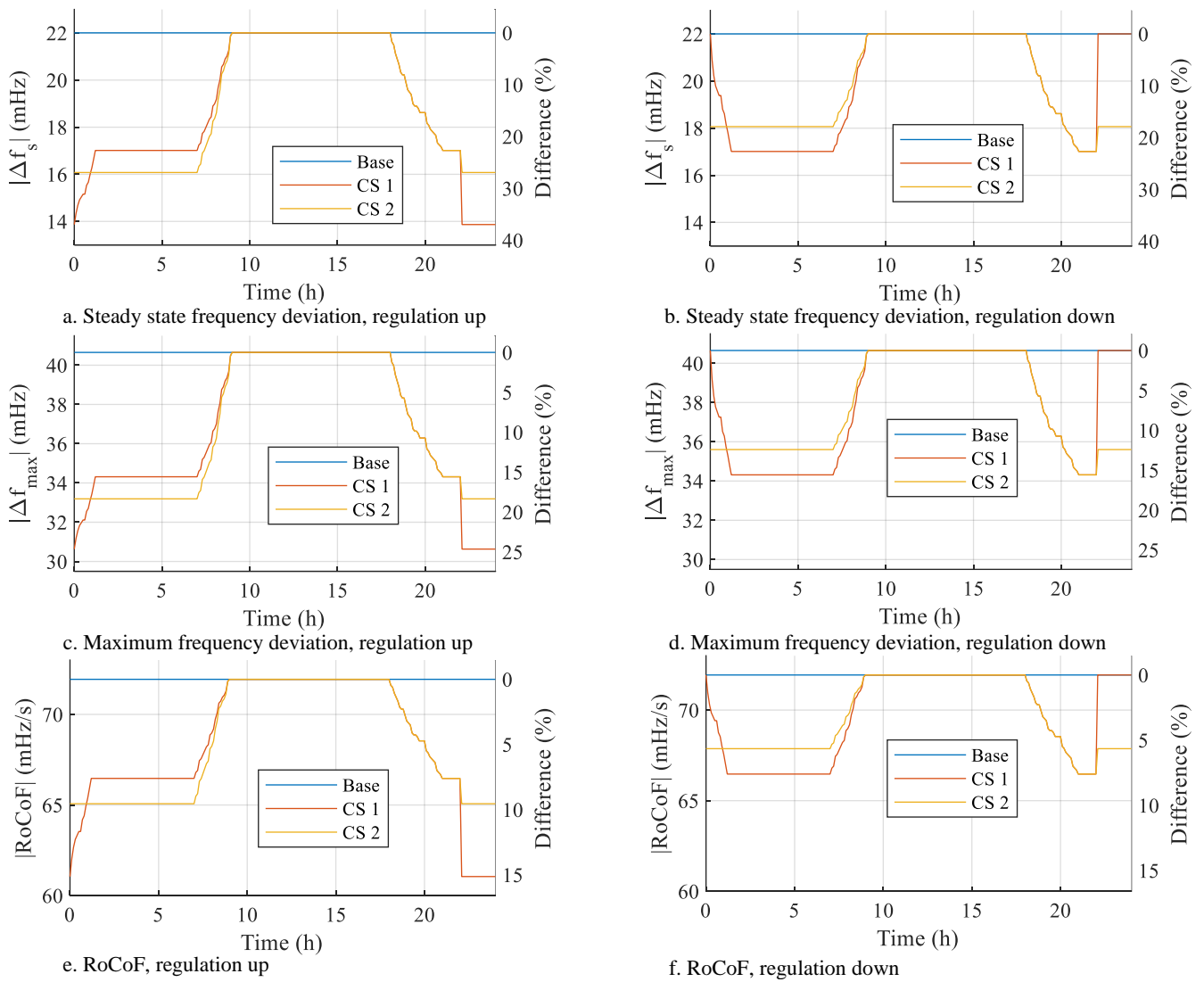


Figure 6. RoCoF, steady state and maximum frequency deviation under 1.5% load perturbation. Both regulation up and down cases are considered for different charging strategies. The results are given for a 24 h period.

strategy. However, the transient response is also very influenced by the dynamics of the systems, which determine the speed of the response. Among all the parameters that determine the dynamics of CGUs and EV fleet, this section is focused on communication delay. This parameter will be highly dependent on the size of the EV fleet, the geographical distribution of the EVs and the communication technology and standard (wireless, optic fibre, PLC, etc.).

The frequency transient responses for an overload of 1.5% considering different time delays  $T_c$  are shown in Figure 7. The simulation is carried out using CS 1 at 5:00. In these conditions, all EVs have a maximum power regulation capability of 10 kW at 0.1 Hz deviation. The base case without EVs is also considered. The  $|RoCoF|$  and  $|\Delta f_{max}|$  improvement are summed in Table 3.

The FFR is highly influenced by the communication delay. The base case RoCoF and maximum deviation could be improved up to a 13.4% and 21.2% without communication delay. However, the RoCoF improvement is nearly halved with a time delay of 0.1 s and it disappears with 0.3 s.  $\Delta f_{max}$  improvement is still feasible with the later delay (>5%).

The communication delay does not only increase RoCoF and  $\Delta f_{max}$ , it also worsens the transient response of the grid compared to the base case. The time needed to damp the power perturbation is considerably increased with a time delay of 0.3 s. A high communication delay in EVs FFR could make the system unstable.

Table 3.  $|RoCoF|$  and  $|\Delta f_{max}|$  results under different  $T_c$  values. Results are also given in % with respect to base simulation.

	$ RoCoF $		$ \Delta f_{max} $	
	mHz/s	Diff (%)	mHz	Diff (%)
Base	71.9	-	40.6	-
$T_c = 0\text{ s}$	62.3	13.4	32.0	21.2
$T_c = 0.1\text{ s}$	66.5	7.5	34.3	15.5
$T_c = 0.3\text{ s}$	71.3	0.8	38.3	5.6

## 5. Conclusions

This paper has analysed the impact that EV fleets could have in the frequency stability of low inertia grids. The main conclusion is that the frequency regulation provided by EVs can improve both static frequency deviation and

transient response. However, the achieved improvement depends mainly on the magnitude and the speed of response of the fleet.

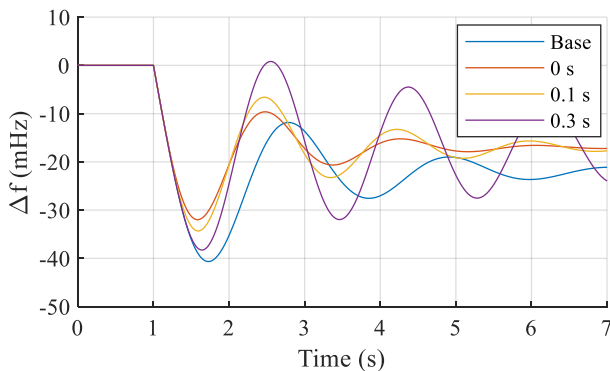


Figure 7. Frequency transient under a 1.5% overload, considering different communication delays.

The magnitude of the response is determined by the availability and charging requirements of the EVs. In this context, the FFR is maximized at nights, when the EVs are plugged into the grid, and minimum along the day. This analysis considers that EVs are not plugged during the day. FFR could be maximized if EVs were connected at public and/or working places. Moreover, the charging strategies lead to different up and down regulation capabilities. The strategy will depend on the market requirements and prices, for which an optimization analysis should be carried out.

The speed of the response in the EV fleet is mainly determined by three elements: the EV dynamics, the frequency measurement dynamics, and the communication delay between EVs and the central controller. This study has focused on the latter, which will depend on the EV fleet size, the geographical dispersion, and the communication technology. The analysis shows that the delay should be minimized to improve the dynamic response. Under high delays, the transient response could worsen and, eventually, it could lead to grid frequency instability.

The current work has focused on the performance of an EV fleet against a single perturbation. As the FFR application time is low, the charge of the EVs has been ignored. For longer regulation period, the state of charge of the EVs should be considered to ensure driving requirements and FFR provision, while reducing battery ageing.

## Acknowledgement

The authors acknowledge the support of the Basque Government (GISEL Research Group) under Grant IT1522-22, Grant KK-2022/00100, as well as the funding from the European Union-Next Generation EU.

## References

[1] P. Scarabaggio, R. Carli, G. Cavone, and M. Dotoli, 'Smart Control Strategies for Primary Frequency Regulation through Electric Vehicles: A Battery Degradation Perspective', *Energies*, vol. 13, no. 17, p. 4586, Sep. 2020.

[2] M. Rezkalla, A. Zecchino, S. Martinenas, A. M. Prostejovsky, and M. Marinelli, 'Comparison between

synthetic inertia and fast frequency containment control based on single phase EVs in a microgrid', *Appl. Energy*, vol. 210, pp. 764–775, Jan. 2018.

[3] Y. G. Rebours, D. S. Kirschen, M. Trotignon, and S. Rossignol, 'A Survey of Frequency and Voltage Control Ancillary Services—Part I: Technical Features', *IEEE Trans. Power Syst.*, vol. 22, no. 1, pp. 350–357, Feb. 2007.

[4] D. Fernández-Muñoz, J. I. Pérez-Díaz, I. Guisández, M. Chazarra, and Á. Fernández-Espina, 'Fast frequency control ancillary services: An international review', *Renew. Sustain. Energy Rev.*, vol. 120, p. 109662, Mar. 2020.

[5] ENTSO-E, 'Technical Requirements for Fast Frequency Reserve Provision in the Nordic Synchronous Area – External document'. 2021.

[6] A. Dik, S. Omer, and R. Boukhanouf, 'Electric Vehicles: V2G for Rapid, Safe, and Green EV Penetration', *Energies*, vol. 15, no. 3, p. 803, Jan. 2022.

[7] K. Sevdari, 'Ancillary services and electric vehicles: An overview from charging clusters and chargers technology perspectives', *Renew. Sustain. Energy Rev.*, 2022.

[8] B. K. Sovacool, J. Kester, L. Noel, and G. Zarazua de Rubens, 'Actors, business models, and innovation activity systems for vehicle-to-grid (V2G) technology: A comprehensive review', *Renew. Sustain. Energy Rev.*, vol. 131, p. 109963, Oct. 2020.

[9] M. Marinelli, K. Sevdari, L. Calearo, A. Thingvad, and C. Ziras, 'Frequency stability with converter-connected resources delivering fast frequency control', *Electr. Power Syst. Res.*, vol. 200, p. 107473, Nov. 2021.

[10] M. T. Muhssin, Z. A. Obaid, K. Al-Anbarri, L. M. Cipcigan, and M. N. Ajaweed, 'Local dynamic frequency response using domestic electric vehicles', *Int. J. Electr. Power Energy Syst.*, vol. 130, p. 106920, Sep. 2021, doi: 10.1016/j.ijepes.2021.106920.

[11] G. Magdy, H. Ali, and D. Xu, 'A new synthetic inertia system based on electric vehicles to support the frequency stability of low-inertia modern power grids', *J. Clean. Prod.*, vol. 297, p. 126595, May 2021, doi: 10.1016/j.jclepro.2021.126595.

[12] ENTSO-E, 'Frequency Measurement Requirements and Usage'. Jan. 29, 2018. [Online]. Available: [https://docstore.entsoe.eu/Documents/SOC%20documents/Regional\\_Groups\\_Continental\\_Europe/2018/TF\\_Freq\\_Meas\\_v7.pdf](https://docstore.entsoe.eu/Documents/SOC%20documents/Regional_Groups_Continental_Europe/2018/TF_Freq_Meas_v7.pdf)

[13] Y. Mu, J. Wu, J. Ekanayake, N. Jenkins, and H. Jia, 'Primary Frequency Response From Electric Vehicles in the Great Britain Power System', *IEEE Trans. Smart Grid*, vol. 4, no. 2, pp. 1142–1150, Jun. 2013.

[14] A. Thingvad, C. Ziras, and M. Marinelli, 'Economic value of electric vehicle reserve provision in the Nordic countries under driving requirements and charger losses', *J. Energy Storage*, vol. 21, pp. 826–834, Feb. 2019.